

Building Floorspace in China: A Dataset and Learning Pipeline

Peter Egger,¹ Susie Xi Rao,² Sebastiano Papini³

¹ Chair of Applied Economics, ETH Zurich; CEPR; CESifo; Leverhulme Centre for Research on Globalisation and Economic Policy (GEP) at the University of Nottingham, Zurich, Switzerland

² Chair of Applied Economics; Institute for Computing Platforms, ETH Zurich, Zurich, Switzerland

³ Chair of Applied Economics, ETH Zurich, Zurich, Switzerland
pegger@ethz.ch, srao@ethz.ch, spapini@ethz.ch

Abstract

This paper provides the first milestone in measuring the floor space of buildings (that is, building footprint and height) and its evolution over time for China. Doing so requires building on imagery that is of a medium-fine-grained granularity, as longer cross-sections and time series data across many cities are only available in such format. We use a multi-class object segmenter approach to gauge the floor space of buildings in the same framework: first, we determine whether a surface area is covered by buildings (the square footage of occupied land); second, we need to determine the height of buildings from their imagery. We then use Sentinel-1 and -2 satellite images as our main data source. The benefits of these data are their large cross-sectional and longitudinal scope plus their unrestricted accessibility. We provide a detailed description of the algorithms used to generate the data and the results. We analyze the preprocessing steps of reference data (if not ground truth data) and their consequences for measuring the building floor space. We also discuss the future steps in building a time series on urban development based on our preliminary experimental results.

1 Introduction

A key challenge in the social sciences dealing with macro- and meso-regional development is that high-quality data one would wish to use in a systematic analysis of the change and development are scarce and spotty. A domain in the limelight of understanding development is the role of agglomeration of people in space – at a macro level between cities and metropolitan areas and their hinterland, and at a meso and micro level within cities and neighborhoods. Measuring agglomeration well at both the macro-, meso-, and micro-levels in space is important for learning about its fundamental role in the course of development, for resource use and saving, for gauging the benefit of infrastructure developments in general and of various types thereof, etc.

However, large sets of data covering many and, ideally all, neighborhoods on various scales and other data to compare with are not always available and if so, then only for where the development process has already matured, namely in industrialized countries such as the United States (McMillen and McDonald 1998; Baum-Snow 2007), Germany (Ahlfeldt et al. 2014), England (Heblich, Redding, and

Sturm 2020). In the light of recent interest in cities in developing countries (Henderson 2002; Tsivanidis 2018; Bryan, Glaeser, and Tsivanidis 2020), one would like to have such data available over a longer time span in countries, which are situated at the steep ascent of the economic growth and catching-up curve, as causation is likely easier to achieve in contexts, where big changes occur and they do so to a sufficiently heterogeneous extent in data that had been collected in a standardized way. The latter is something this paper aims at accomplishing by utilizing modern methods in computer vision in conjunction with satellite imagery in remote sensing from various sources over several years on the housing stock in a large number of cities in China.

China is an economy that fits the purpose very well. To start with, it grew at a much faster rate than the data-rich industrialized countries since its opening up to foreign trade in 1978. Hence, it grew very rapidly within a time span, when remote sensing data are available. Second, it has undergone a substantial structural change from an agricultural economy to one of the leading manufacturers on the globe and, more recently, a big surge in certain services, as is suggested by the change in the overall as well as the field-specific enrollment rates at its universities. Going hand in hand with structural change, the country witnessed a transformation in the distribution of its population between rural areas and agglomerations (cities and metropolitan areas). The latter is partly reflected in a string of reforms of the household registration system (called *hukou*), which essentially grants legal access to home ownership, education, or the health system, but also beyond (e.g., in terms of illegal migrant work in agglomerations, which is to a certain extent tolerated by the authorities as long as it benefits the economy). Hence, over the past four decades a large surge on the demand and supply of floor space in Chinese cities emerged.

When speaking of agglomeration, demographers and other social scientists typically think of the density of people in space. In most economies and jurisdictions, detailed data on the residents in meso or micro space turn are surprisingly scarce, and they can often only be garnered from sources where households somehow disclose their presence (e.g., official work records, official purchases of homes, etc.). Yet, even in the United States, an illegal migrant could work on the black market and rent a home without going on record regarding their residence, and in some agglomerations the

mass of off-record individuals might be non-trivially large. Moreover, one might speak of agglomerations from the viewpoint of production, and then the space occupied by it would be of interest. In that case, official data might also be problematic for a host of reasons. For example, register data of companies typically list the parent company and its address. This is exactly problematic for those companies that are said to account for the lion’s share in production, namely multi-plant and –site units. Also, such records may list the core activity. However, with large manufacturing companies, for example, the headquarters are often in city centers, while the production operations are in the outskirts or the hinterland of cities. The latter suggests that production-related agglomeration aspects are likely mismeasured, as are residence-related agglomeration aspects of households. Altogether, this creates a demand for an alternative route of measurement for the agglomeration phenomenon.

This paper provides a first milestone in this context by delivering a rich dataset on building-specific floorspace (that is, building footprint and height) and its evolution over time for China. Moreover, we build a pipeline to collectively learn building footprint and height in a single multi-class object segmenter. The **challenges** of this attempt are the following.

1. **Data sources and collection.** Imagery of buildings at a high resolution only exist for selected cities if not subregions within them and often require researchers to perform substantial pre-processing in both ground truth and satellite images. The quality of such pre-processing certainly impacts the detection results. Additionally, one needs to discuss the cross-sectional combination and time-series concatenation of several sources of satellite imagery to produce consistent data panels that are longer than life-cycles of satellites.
2. **Ensemble approach to learn building footprint and height.** Deep learning methods have fundamentally transformed the approaches of people to use remote sensing data. Specific application and architecture of how to collectively learn footprint and height with multi-task learning or with a two-stage setting will be discussed.
3. **Evaluation of prediction quality.** How to quantify the quality of the prediction and to understand the predictions empirically remains a question.

As a first step, the paper delivers a rich dataset on the expansion of China’s floor space. We collect satellite data from several sources in 27 cities at the scale of 10x10 meters. We then use a multi-class segmenter approach to gauge the building footprint and height in the same framework: first, we determine whether a surface area is covered by buildings (the square footage of occupied land); second, we determine the height of buildings from their imagery. The predictions of these two outcomes, together with established algorithms (U-Net: Ronneberger, Fischer, and Brox (2015)) to determine the floor space of buildings by their volume, provide a specific estimate of the floor space of buildings. Our codebase is publically accessible under <https://gitlab.ethz.ch/mujiang/building-floorspace-china>.

Contribution. We provide a detailed description of the algorithms used to generate the data and result. We have also

analyzed the preprocessing steps of “reference data” (if not ground truth data) and their consequences on learning about the building floor space. We indicate in a summary how these data can be used to analyze microregional agglomeration patterns within cities (e.g., speaking to the question of mono- versus polycentric structures of cities), the role of infrastructure in stimulating and sustaining the distribution of floorspace, and the distribution of private versus business floorspace occupation, the distribution of work altogether as well as by macro sector occupation (service versus production in manufacturing), as well as the distribution of average incomes between agglomerations of different types.

One of the merits of the proposed approach will be that it can be used in conjunction with medium-resolution remote-sensing data that permit tracking changes in floor space for longer time windows. The latter is elemental not only for assessing hypotheses in urban (related to the determinants as well as the effects of agglomeration on economic outcome) and public economics (related to the effects of infrastructure developments and agglomeration) economics but also for statistics and econometrics, if identification of the relationships and of causal effects is sought from changes in the data rather than from cross-sectional states thereof.

2 Building footprint recognition and building height estimation

2.1 Data preparation

We obtain the Sentinel satellite imagery as our main data source and benefit from its free and open policy. The image sets include both Sentinel-1 (Synthetic-aperture radar, SAR) and Sentinel-2 (multi-spectral optical) products which both provide near global coverage and high spatial resolution. We implement the images processing and downloading through Google Earth Engine API, and a total of 27 cities¹ are selected among our ground truth data. The areas of interest for each city are acquired from the crowd-sourced dataset used in earlier work, such as Cao and Huang (2021).

For Sentinel-2 optical images, we select the level 2A product which provides orthoimage Bottom-Of-Atmosphere (BOA) corrected surface reflectance data. The bands we used contain B2 (blue), B3 (green), B4 (red), and B8 (NIR), with a spatial resolution of 10x10 meters. To reduce the impacts of cloud occlusion, we first filter out images with more than 60% cloud coverage and further apply the cloud mask by making use of the additional Sentinel-2 cloud probability image collections.² We query the data based on the above condition from 2017 to 2022 and take the mean values from multiple returned images to get a single image for each year, covering the area of interest for each city.³

¹The 27 cities in our samples are Baoding, Cangzhou, Foshan, Hohhot, Jiaying, Langfang, Linyi, Nanchang, Qinhuangdao, Shengyang, Shenzhen, Suzhou, Taizhou (Zhejiang), Taiyuan, Tangshan, Weifang, Wuhu, Wuxi, Xi’an, Xuzhou, Yangzhou, Yantai, Yinchuan, Zaozhuang, Zhenjiang, Zhongshan and Zhuhai.

²See <https://developers.google.com/earth-engine/tutorials/community/sentinel-2-s2cloudless>.

³Note that the results we report in Section 3 are obtained using satellite images from 2017, as it is conjectured that the crowd-

For Sentinel-1 radar images, we select VV and VH polarizations acquired from a C-band SAR sensor with combined ascending and descending orbit directions to collect maximum information content. Data are queried over the years from 2015 to 2022, and for each year, the same image collections reduction technique as Sentinel-2 is applied.

2.2 Method: multi-class object segmenter

We adopted U-Net, a convolutional neural network that uses skip connections between the encoder and the decoder, as our semantic segmentation architecture. We illustrate our architecture in Figure 1. It was originally developed for biomedical image segmentation (Ronneberger, Fischer, and Brox 2015), and became later popular in urban studies for land cover classification or for the extraction of roads or buildings from satellite imagery (c.f. Li et al. (2021)).

We have evaluated the data quality after the ground truth calibration introduced in Section 2.1. 27 of 77 cities have apparent higher data quality, which could be due to the building directions (north-south vs. northwestern-southeastern) or due to the quality of crowdsourcing. We used the data of these 27 cities as input, which equates to 17'163 images after splitting each image into 64×64 tiles. We filter out tiles with less than 10% of pixels in the tiles. The train/validation/test split ratio is 80%/10%/10%. In addition to the stride sizes illustrated in Figure 1, the other hyperparameters of U-Net are dynamic learning rates starting with 0.001. The loss function is a weighted dice coefficient in which the weight of the non-building class is set as 10% of other building classes to address the class imbalance issue.⁴ We benchmark our algorithm in a machine with 64 units of AMD EPYC 7313 16-Core Processor, 504 GB memory, and a single unit of GPU (NVIDIA GeForce RTX 3090, 24GB memory), and the training time is 11 seconds per epoch on average. We train the U-Net for 80 epochs. Three random seeds are selected, and we report the averaged performance metrics.

We learn the building footprint and height in one model. For footprint, we predict if the area of interest is covered by building or non-building. For building height, we learn the height conditioned on the fact that the area is covered by buildings or not. We have four classes in the *softmax* function, that is, no building, buildings with a height of below 6 meters, 6 to 27 meters and above 30 meters.⁵ These cutoffs are chosen to slice the multi-modal distribution of building heights in all 77 cities in the crowd-sourced dataset into three categories of a local maximum (52%, 39%, 8%).

sourced ground truth is from 2017. We will use 2017-2022 in future work in a similar setting, especially when we have better quality ground-truth data collected, as discussed in Section 5.

⁴In future work, we plan to benchmark the effect of class weights on the prediction quality. It is also interesting to compare the sliding window solution vs. static split of 64×64 tiles, because the non-building class might vary largely depending on how we split the image.

⁵We have tested different cutoff values, e.g., below 10 meters, 10 to 20 meters, above 20 meters, the results are very close, though.

3 Results and Evaluation

3.1 Quantitative analysis

We have carried out experiments with different setups to predict footprint and height as shown in Table 1: (a) Sentinel-1 (SAR data), (b) Sentinel-2 (optical images), and (c) Sentinel 1+2 (the overlay of Sentinel-1 and -2).

The evaluation metrics that we use are accuracy, precision, and recall. Accuracy measures how well we predict all the classes (non-buildings, buildings and their heights); precision and recall are calculated only on the true positives (buildings and their heights). For building footprint, we quantify the performance on the pixel level. The true positive is computed with the IoU score (intersection of the union between predicted and true areas) being $\geq 50\%$. For learning height, we take the class with the highest probability after the *softmax* transformation. If two classes are in a tie, we always choose the class that is higher in rank. We see that combining SAR data with optical images in (c) gives us the best performance in all metrics.

Discussion. A natural extension of the current approach would be to perform a two-stage modeling as Wen et al. (2019), which uses a commercial data set of multi-view images from the ZY-3 satellite, allowing for a 3D modeling of the building space. Cao and Huang (2021) who study 42 Chinese cities, they also have access to sources identical to Wen et al. (2019) and learn the exact heights of the buildings. However, our goal of this project is to use an open-source platform and a simple pipeline that can benefit the synergy of remote sensing and urban economics. Note that these multi-view images are not publicly available and are expensive to acquire, while our goal in this project is to utilize open source data. Besides, the key difference between their approaches and ours is that we combine the learning of the building footprint and building heights in one multi-class object segmenter. In the absence of multi-view imagery, our hypotheses are as follows in two-stage models. Our one-stage implementation is more efficient; the performance of two-stage models will not vary much. As a robustness check, we conducted two-stage experiments on the best setup (c), the results of which substantiate our claims. In Appendix B, we present the experimental setup and results.

3.2 Case studies

To further gauge the quality of our segmenter compared to crowd-sourced ground truth, we manually analyzed 100 randomly selected images from the data source. We categorize the predictions made by our segmenter (with Sentinel 1+2) into four types: (C1) predictions matched well with ground truth; (C2) poor quality of ground truth (predictions are seemingly closer to the satellite images);⁶ (C3) we cannot judge the predictions/ground truth based on the quality of the satellite images; (C4) our segmenter performs poorly. Among these images, the types (C1) - (C4) represent 37%, 21%, 9%, and 33%, respectively. In Appendix C, we list an example for each type in Figure 2 in Appendix A. The three

⁶It could also be due to the temporal difference between the ground truth and remote sensing image, considering the exact time when the ground truth data was obtained is uncertain.

	(a) Sentinel-1			(b) Sentinel-2			(c) Sentinel 1+2		
	Accuracy	Precision	Recall	Accuracy	Precision	Recall	Accuracy	Precision	Recall
Footprint	0.722	0.320	0.598	0.741	0.336	0.560	0.762	0.375	0.617
Height	0.670	0.194	0.364	0.703	0.229	0.382	0.724	0.261	0.449

Table 1: U-Net performance metrics with Sentinel-1 and -2.

classes of building heights are colored red ($\leq 6\text{m}$), green ($9 - 27\text{m}$), and blue ($\geq 30\text{m}$), respectively.

4 Related work

Here, we summarize the relevant works in the domain of remote sensing that have inspired our contribution.

2D-mapping. Remote sensing methods of various kinds have been in use for a long time in earth science disciplines such as ecology, glaciology, and geology since the start of the first Landsat missions 1972. In the 2000s, thanks to increased data quality and artificial intelligence methods, renewed interest in remote sensing for urban structures had arisen. It became increasingly possible to map the whole globe in land use categories, although in a relatively low resolution of 500 meter cells (Schneider, Friedl, and Potere 2010). This tradition is interested in mapping different land use types where urban use is just one among others. This resolution was increasingly refined to 13 meters (Esch et al. 2017) and 10 meters (Gong et al. 2019) for global mappings. At this granularity, individual buildings become visible, and we can speak of building footprints more akin to a traditional map than land use classifications. While classification in the former research is based on unsupervised learning methods and a random forest framework in the latter, Wu et al. (2021) provide building footprint mappings of China based on a U-Net deep learning architecture.

Building height estimation. In the last few years a new strand of this literature has emerged, which estimates building height, as well as land use categories. In this context, the height of buildings measures the intensity of land use. Li et al. (2020) create a 3D continental mapping of North America, Europe, and China using a random forest model. The main input sources for this estimation are Landsat 8 (optical) and Sentinel-1 (SAR) and the final data set has a resolution of roughly 1km^2 . Frantz et al. (2021) use a support vector machine method based on Sentinel-1 (SAR) and Sentinel-2 (optical). The idea is to combine building height estimation based on shadow length and radar reflectance. The result of the latter project is a national map of Germany with a 10m resolution. Cao and Huang (2021) build on vastly superior multi-view image data from the Chinese Ziyuan-3 satellite. Using a deep learning methodology, they produce a 3D mapping with a 2.5-meter resolution for a set of 42 Chinese cities. Yet, neither the satellite imagery nor the resulting mapping are available on open source bases. Further recent contributions that have looked at building height estimation in China include Ji and Tang (2020), Yang and Zhao (2022) and Yang and Zhao (2022). Yu et al. (2021) generate a panel of building heights for Shenzhen that runs from 1986 to 2017. They start from a high-resolution Light

Detection and Ranging (LiDAR) map, and reversely update with low-resolution Landsat archive imagery.

5 Discussion, future work, and conclusion

Discussion: data quality. Using data of a meso-grained resolution of 10m provides an advantage of large cross-sectional and time-series coverage. However, it comes at an inevitable cost of precision. At this stage, we provide our dataset and pipeline as an open-sourced platform. However, in the future, we will harmonize various satellite images incl. Planet, which would substantially increase building visibility.⁷

Discussion: better ground truth of building footprint and height. Our team is actively developing a tool that crawls the up-to-date Amap 3D reconstruction.⁸ We provide a short illustration of our tool in Appendix D. This set of ground truth should be of better quality and can hence save the efforts we need spend on annotating images without ground truth data.

Discussion: annotation. The idea is that for areas of interest without ground truth data (via Amap), we need to acquire human annotations. We are in contact with professionals who are experienced in satellite image annotations. We can benefit from their expertise and tool designed to annotate forest data.⁹

Discussion: robustness checks. We will carry out robustness checks at an aggregate level with demographic indicators of cities in census data, for example, building coverage in a county/city. We also plan to conduct a correlation analysis with nightlight data to gauge the prediction quality.

Conclusion. This paper provides a first milestone in generating a panel dataset of urban development, a rich dataset on building-specific floorspace (that is, building footprint and height), and its evolution over time for China. the key goal is to cover many cities across China and a long time span. We build a pipeline to collectively learn building footprints and heights in a single multi-class object segmenter. We have also analyzed the preprocessing steps of reference data (if not ground truth data) and their consequences on learning about the building floor space. Our paper lays the groundwork for further empirical research that builds on the theoretical foundation of quantitative urban economic models.

⁷Our team is supported by ETH Zurich library which has acquired an academic licence from Planet Labs PBC. We cannot open-source the Planet images, but we are willing to provide pre-trained models trained by harmonized Planet + Sentinel images.

⁸See <https://lbs.amap.com/demo/javascript-api/example/3d/fixed-view> for an official static demo provided by Amap.

⁹Our contacts at Restor, see <https://restor.eco/about/team/>.

A U-Net architecture

We illustrate in Figure 1 the U-Net architecture in our multi-class object segmenter.

B Robustness check with two-stage models

To validate the robustness of our proposed one-stage model, we have tested two-stage models with Sentinel 1 + 2 images. In the two-stage models, we first predict only the footprints of the buildings (the first stage) and then feed the predicted footprints into a height prediction model (the second stage). We have validated three architectures in the second stage of the two-stage models when predicting heights: (A1) stacking the building footprint prediction results and the Sentinel images together as height prediction model inputs; (A2) clipping Sentinel images with building footprint prediction results before putting them into the height prediction model; (A3) training in parallel the building footprint prediction and height prediction in the encoder part, and use skip connection to concatenate them for the bottleneck and decoder parts of the U-Net model as in Cao and Huang (2021). The first stage (footprint prediction) is identical among these three architectures. The loss and activation functions of each stage are similar to those used in the one-stage model; *sigmoid* and *softmax* as activation for footprint and height predictions, respectively; the loss function remains the weighted dice coefficient.

The results of the two-stage models show a slight increase in the prediction of building footprints, as we see in Table 2, but the height prediction performance remains almost the same for all of our attempts. The first stage (footprint) prediction takes 10 seconds on average per epoch, while A1, A2 and A3 take 17.5, 20, 18.75 seconds, respectively, in the second stage (height prediction). Compared to our segmenter (with 11 seconds per epoch), which learns the footprint and height in a one-stage model, the computational cost of two-stage models is substantially higher.

There is still room for improvement in height prediction, which requires input from remote sensing theory. On the one hand, it could help to integrate indices based on spectrum knowledge such as the Morphological Building Index (MBI) and the Normalized Difference Vegetation Index (NDVI), so that the texture of buildings could be better represented and recognized. On the other hand, analyzing the physical properties of buildings in remote sensing images, such as shadow and the inclination angle of SAR data, could further improve the prediction performance.

	(c) Sentinel 1+2						
	Footprint			Height			
	Accuracy	Precision	Recall	Accuracy	Precision	Recall	F1_micro
One-stage	0.762	0.375	0.617	0.724	0.261	0.449	0.330
Two-stage (A1)				0.726	0.261	0.433	0.326
Two-stage (A2)	0.773	0.442	0.673	0.725	0.253	0.428	0.318
Two-stage (A3)				0.725	0.266	0.446	0.333

Table 2: Robustness check of U-Net performance metrics with Sentinel 1+2 in two-stage models.

C Case studies of prediction results

In Figure 2, we show four examples of the prediction results. More examples and our annotation protocol can be found in our project repository following this link <https://gitlab.ethz.ch/mujiang/building-floorspace-china>.

D Better ground truth with Amap

Figure 3 is a screenshot of our customizable tool built on top of Amap’s API. By querying a polygon json, we obtain the actual footprint ground truth provided by Amap. In Figure 4, we contrast the ground truth provided by the actual Amap (in black) and the ground truth in the crowd-sourced dataset (in red, supposedly from about 2017). These two sets of reference data are overlaid on top of a satellite image of the latest high-resolution image of a sampled area. The two satellite images used here are provided by Amap in the period 2021-2022. According to Amap, the source is DigitalGlobe&spaceview, with and update frequency 0.5-1 year for urban areas, longer for remote areas. As we can see in the mismatched area, the actual ground truth data seem to better represent the building coverage. In future work, we will systematically evaluate the quality of various reference data. Moreover, we also see some areas of interest where no reference data is available; therefore, minimal human efforts to encoding are expected to bring benefits as we discussed in Section 5.

Acknowledgements

We sincerely thank our research assistants Yuru Jia and Muyang Jiang for providing excellent support throughout the project. Special thanks go to our friends David Dao at GainForest/DS3Lab and Dr. Josh Veitch Michaelis at Restor/DS3Lab, for their inspirational discussions and brainstorming sessions.

References

- Ahlfeldt, G.; Redding, S.; Sturm, D.; and Wolf, N. 2014. The Economics of Density: Evidence from the Berlin Wall. NBER Working Papers 20354, National Bureau of Economic Research, Inc.
- Baum-Snow, N. 2007. Did Highways Cause Suburbanization? *The Quarterly Journal of Economics*, 122(2): 775–805.
- Bryan, G.; Glaeser, E.; and Tsivanidis, N. 2020. Cities in the Developing World. *Annual Review of Economics*, 12(1): 273–297.
- Cao, Y.; and Huang, X. 2021. A deep learning method for building height estimation using high-resolution multi-view imagery over urban areas: A case study of 42 Chinese cities. *Remote Sensing of Environment*, 264: 112590.
- Esch, T.; Heldens, W.; Hirner, A.; Keil, M.; Marconcini, M.; Roth, A.; Zeidler, J.; Dech, S.; and Strano, E. 2017. Breaking new ground in mapping human settlements from space – The Global Urban Footprint. *ISPRS Journal of Photogrammetry and Remote Sensing*, 134: 30–42.

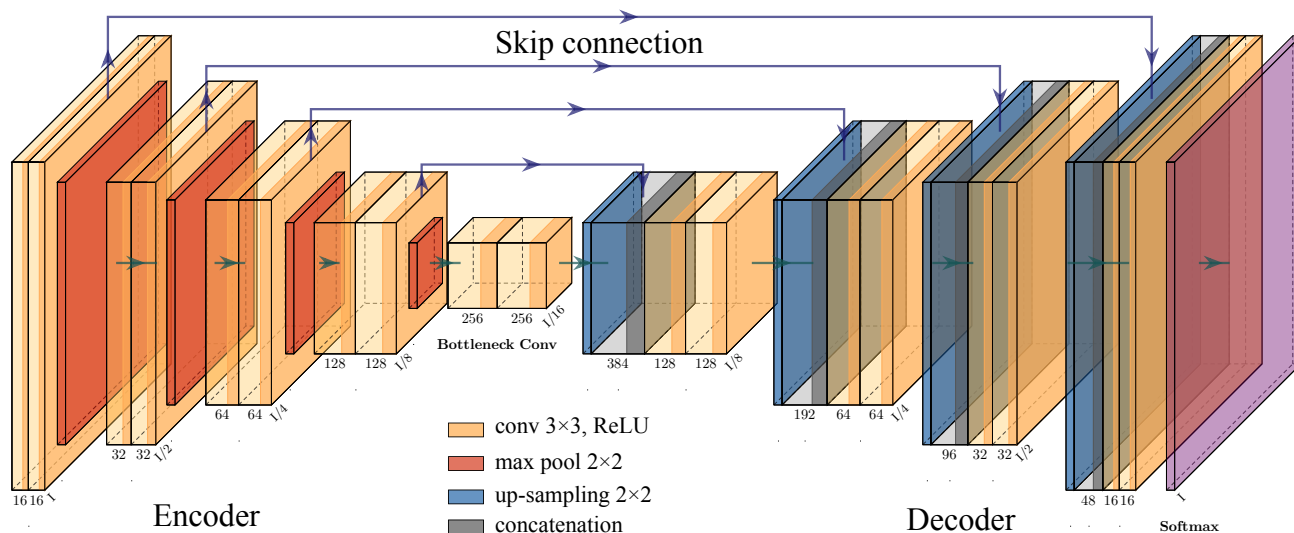


Figure 1: U-Net architecture of our multi-class object segmenter.

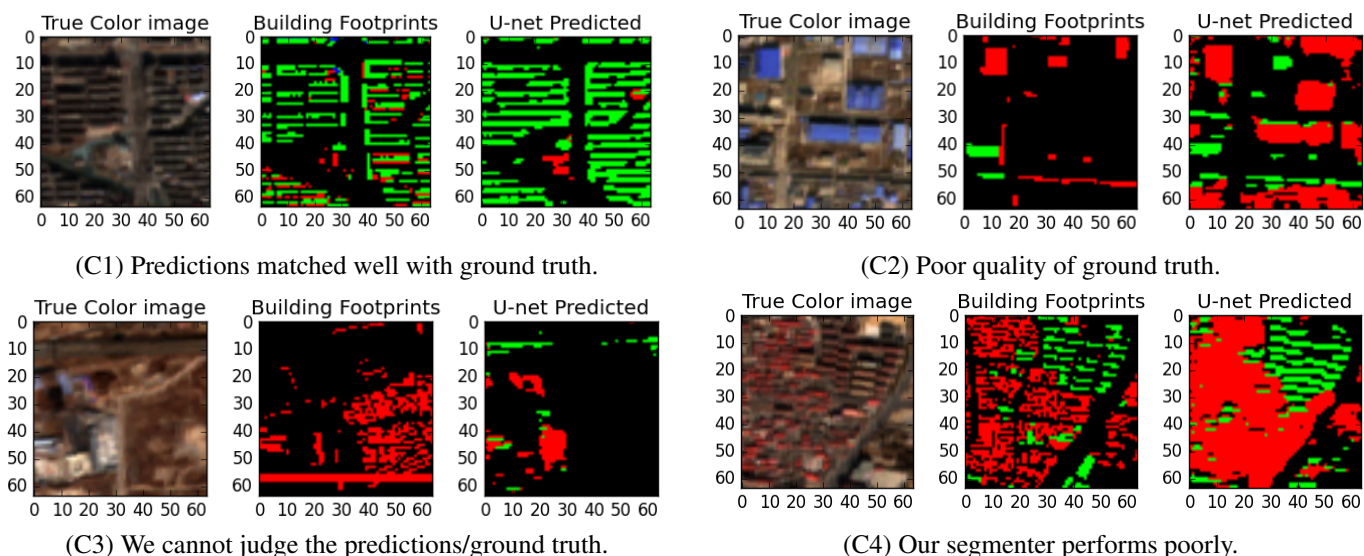


Figure 2: Case studies of Sentinel-2 satellite images, ground truth, and predicted areas. black/red/green/blue: no building, $\leq 6m$, 6-27m, $\geq 30m$.

Frantz, D.; Schug, F.; Okujeni, A.; Navacchi, C.; Wagner, W.; van der Linden, S.; and Hostert, P. 2021. National-scale mapping of building height using Sentinel-1 and Sentinel-2 time series. *Remote Sensing of Environment*, 252: 112128.

Gong, P.; Liu, H.; Zhang, M.; Li, C.; Wang, J.; Huang, H.; Clinton, N.; Ji, L.; Li, W.; Bai, Y.; Chen, B.; Xu, B.; Zhu, Z.; Yuan, C.; Ping Suen, H.; Guo, J.; Xu, N.; Li, W.; Zhao, Y.; Yang, J.; Yu, C.; Wang, X.; Fu, H.; Yu, L.; Dronova, I.; Hui, F.; Cheng, X.; Shi, X.; Xiao, F.; Liu, Q.; and Song, L. 2019. Stable classification with limited sample: transferring a 30-m resolution sample set collected in 2015 to mapping 10-m resolution global land cover in 2017. *Science Bulletin*,

64(6): 370–373.

Heblich, S.; Redding, S. J.; and Sturm, D. M. 2020. The Making of the Modern Metropolis: Evidence from London*. *The Quarterly Journal of Economics*, 135(4): 2059–2133.

Henderson, V. 2002. Urbanization in Developing Countries. *The World Bank Research Observer*, 17(1): 89–112.

Ji, C.; and Tang, H. 2020. Number of Building Stories Estimation from Monocular Satellite Image Using a Modified Mask R-CNN. *Remote Sensing*, 12(22).

Li, C.; Fu, L.; Zhu, Q.; Zhu, J.; Fang, Z.; Xie, Y.; Guo, Y.; and Gong, Y. 2021. Attention Enhanced U-Net for

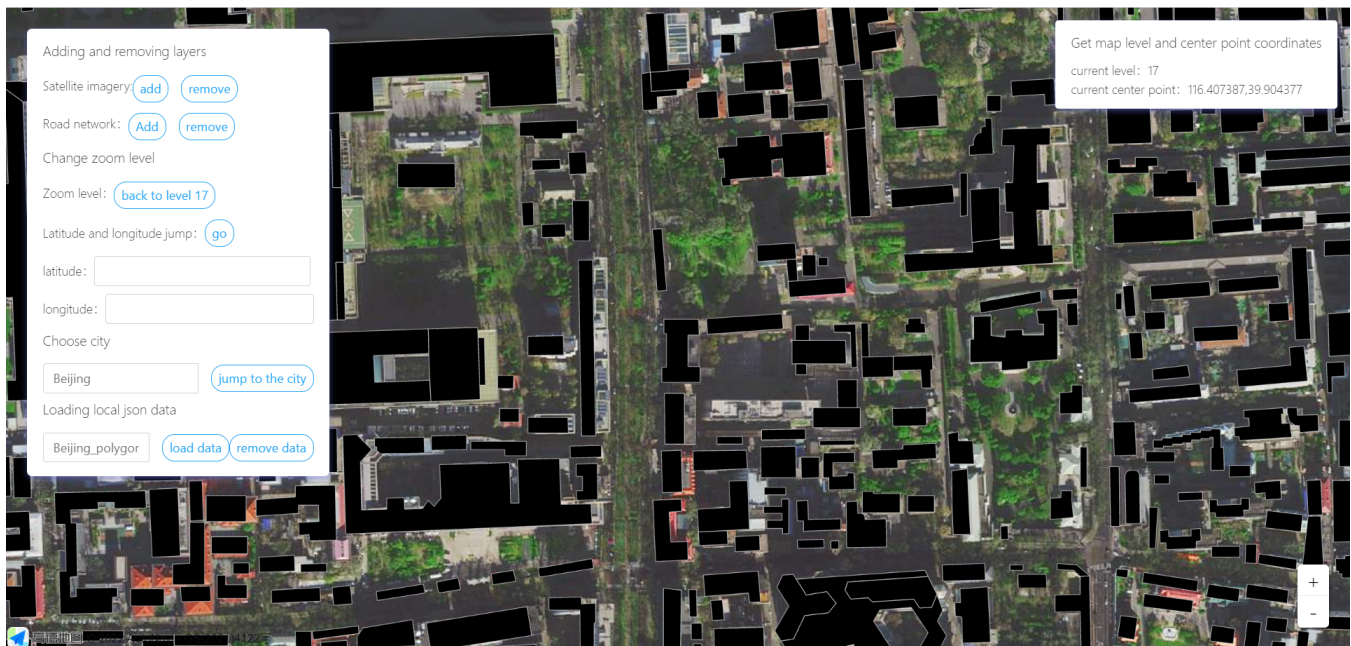


Figure 3: Customized toolbox for accessing Amap’s building footprint and satellite imagery dataset, built on Amap’s API.

Building Extraction from Farmland Based on Google and WorldView-2 Remote Sensing Images. *Remote Sensing*, 13: 4411.

Li, M.; Koks, E.; Taubenböck, H.; and van Vliet, J. 2020. Continental-scale mapping and analysis of 3D building structure. *Remote Sensing of Environment*, 245: 111859.

McMillen, D. P.; and McDonald, J. F. 1998. Population Density in Suburban Chicago: A Bid-rent Approach. *Urban Studies*, 35(7): 1119–1130.

Ronneberger, O.; Fischer, P.; and Brox, T. 2015. U-net: Convolutional networks for biomedical image segmentation. In *International Conference on Medical image computing and computer-assisted intervention*, 234–241. Springer.

Schneider, A.; Friedl, M. A.; and Potere, D. 2010. Mapping global urban areas using MODIS 500-m data: New methods and datasets based on ‘urban ecoregions’. *Remote Sensing of Environment*, 114(8): 1733–1746.

Tsivanidis, J. N. 2018. The Aggregate and Distributional Effects of Urban Transit Infrastructure: Evidence from Bogotá’s TransMilenio.

Wen, D.; Huang, X.; Zhang, A.; and Ke, X. 2019. Monitoring 3D building change and urban redevelopment patterns in inner city areas of Chinese megacities using multi-view satellite imagery. *Remote Sensing*, 11(7): 763.

Wu, F.; Wang, C.; Zhang, H.; Li, J.; Li, L.; Chen, W.; and Zhang, B. 2021. Built-up area mapping in China from GF-3 SAR imagery based on the framework of deep learning. *Remote Sensing of Environment*, 262: 112515.

Yang, C.; and Zhao, S. 2022. A building height dataset across China in 2017 estimated by the spatially-informed approach. 9(1): 76.

Yu, W.; Jing, C.; Zhou, W.; Wang, W.; and Zheng, Z. 2021. Time-Series Landsat Data for 3D Reconstruction of Urban History. *Remote Sensing*, 13(21).

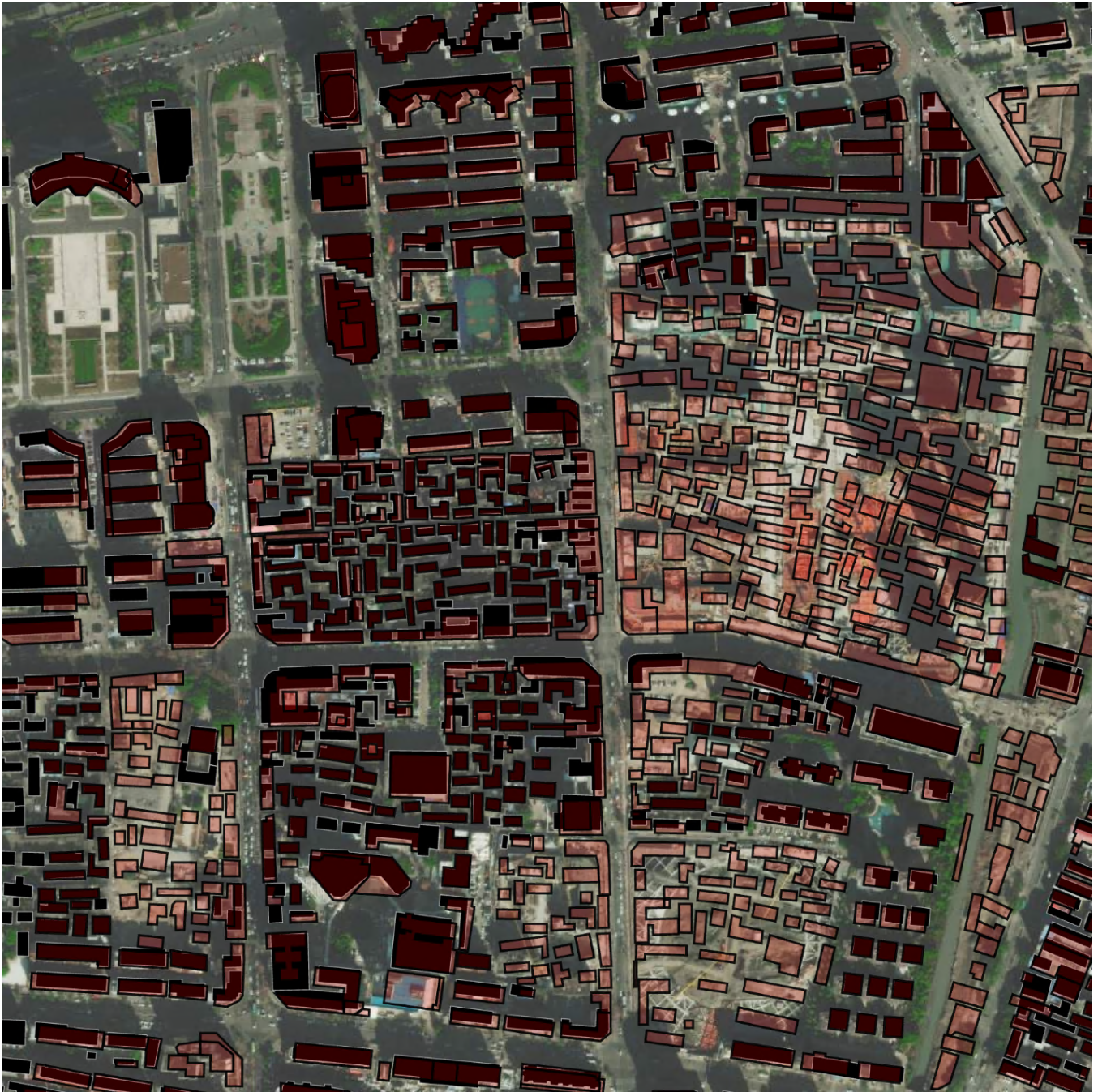


Figure 4: Comparison of the building footprint in crowd-sourced dataset (red) and up-to-date Amap dataset (black).